Acta Crystallographica Section F
Structural Biology and Crystallization Communications
ISSN 1744-3091

Production, purification, crystallization and preliminary X-ray diffraction studies of the nucleoside diphosphate kinase b from *Leishmania major*

Celisa Caldana Costa Tonoli,[a] Plinio Salmazo Vieira,[b] Richard John Ward,[b] Raghuvir Krishnaswamy Arni,[c] Arthur Henrique Cavalcante de Oliveira[b] and Mario Tyago Murakami[a]*

[a]Center for Structural Molecular Biology, Brazilian Association for Synchrotron Light Technology, Campinas-SP, Brazil, [b]Department of Chemistry, FFCLRP-USP, Ribeirão Preto-SP, Brazil, and [c]Department of Physics, IBILCE/UNESP, São José do Rio Preto-SP, Brazil

Correspondence e-mail: mtmurakami@lnls.br

Received 13 August 2009
Accepted 16 September 2009

Nucleoside diphosphate kinases (NDKs; EC 2.7.4.6) play an essential role in the synthesis of nucleotides from intermediates in the salvage pathway in all parasitic trypanosomatids and their structural studies will be instrumental in shedding light on the biochemical machinery involved in the parasite life cycle and host–parasite interactions. In this work, NDKb from *Leishmania major* was overexpressed in *Escherichia coli*, purified to homogeneity and crystallized using the sitting-drop vapour-diffusion method. The NDK crystal diffracted to 2.2 Å resolution and belonged to the trigonal crystal system, with unit-cell parameters $a = 114.2$, $c = 93.9$ Å. Translation-function calculations yielded an unambiguous solution in the enantiomorphic space group $P3_221$.

1. Introduction

Nucleoside diphosphate kinases (NDKs) are ubiquitous enzymes that are crucial for the maintenance of intracellular nucleoside triphosphate (NTP) levels and catalyze the transfer of the γ-phosphoryl group from an NTP to a nucleoside diphosphate (NDP) by a ping-pong mechanism involving a phosphohistidine intermediate (Parks & Agarwal, 1973; Lascu *et al.*, 2000). These enzymes provide NTPs for nucleic acid synthesis, cytidine triphosphate (CTP) for lipid synthesis, uridine-5′-triphosphate (UTP) for polysaccharide synthesis and guanosine-5′-triphosphate (GTP) for protein elongation, signal transduction and microtubule polymerization. Additional functions have been ascribed to NDK in different organisms, including regulation of gene expression in mammalian cells (Postel, 2003), participation in the purine-salvage pathways of trypanosomatid protozoa (Landfear *et al.*, 2004) and bacterial pathogenesis (Chakrabarty, 1998). In protozoan parasites, NDK has been reported to be involved in the salvage pathway in which free purines are converted to nucleosides and subsequently to nucleotides (Marr, 1991).

NDK has been described as a secreted protein from intracellular pathogens that may act as a modulator of macrophage apoptosis by interacting with P2Z receptors. The NDK of *Mycobacterium bovis* extended the life of macrophages by the sequestration of extracellular ATP from P2Z receptors (Zaborina *et al.*, 1999). Furthermore, extracellular secretion of NDK has been reported in *Pseudomonas aeruginosa* (Shankar *et al.*, 1996), *Vibrio cholerae* (Punj *et al.*, 2000) and *Trichenella spiralis* (Gounaris *et al.*, 2001). NDKb has been identified as an abundant component in the subproteomic analysis of the microsomal fraction of *Leishmania major* promastigotes (de Oliveira *et al.*, 2006). Recently, both secreted native and recombinant *L. amazonensis* NDK have been found to prevent ATP-induced cytolysis of J774 macrophages *in vitro*, suggesting that NDK not only conducts its normal housekeeping functions but can also preserve host-cell integrity for the benefit of the parasite (Kolli *et al.*, 2008).

Several crystal structures of NDK from bacteria (Misra *et al.*, 2009), mammals (Lacombe *et al.*, 1991) and viruses (Jeudy *et al.*, 2009) have been reported and they share around 44% sequence identity. The main structural difference resides in their oligomeric states, which can either be a dimer, a trimer or a hexamer. Despite the importance of NDK in the life cycle of trypanosomatids, no crystal

Table 1
Data-processing and molecular-replacement statistics.

Values in parentheses are for the highest resolution shell.

Data processing	
Data-processing software	*HKL*-2000
Space group	$P3_221$
Unit-cell parameters (Å)	a = 114.2, c = 93.9
Matthews coefficient (Å^3 Da^{-1})	3.16
Solvent content (%)	61.06
No. of molecules in the asymmetric unit	3
No. of unique reflections	36081
No. of observed reflections	211450
Redundancy	5.9 (4.9)
Resolution range (Å)	50.0–2.18 (2.26–2.18)
Completeness (%)	96.4 (91.2)
$R_{\rm merge}$† (%)	8.3 (23.1)
$\langle I/\sigma(I)\rangle$	19.28 (5.26)
Wilson B factor (Å^2)	31.25
Molecular replacement	
Overall correlation coefficients (%)	
Rotation function	11.5
Translation function	35.9
Refine fitting	45.1
Rigid-body refinement R factor (%)	39.4

† $R_{\rm merge} = \sum_{hkl}\sum_i |I_i(hkl) - \langle I(hkl)\rangle| / \sum_{hkl}\sum_i I_i(hkl)$, where $I_i(hkl)$ is the ith observation of reflection hkl and $\langle I(hkl)\rangle$ is the weighted average intensity for all observations i of reflection hkl.

structure of an NDK has been solved from *Leishmania* or any other trypanosome. This work represents the first structural report of an NDK from a parasitic trypanosomatid.

The key role of NDKb in trypanosomatid purine metabolism and its possible effect in prolonging the life of the host cell in *Leishmania* infection indicates that the enzyme is a promising target for functional and structural investigations and may help in understanding of the biology of the parasite and thereby contribute to the development of new strategies for the treatment of leishmaniasis. In this work, we present the expression, purification, crystallization and preliminary X-ray crystallographic analysis of NDKb from *L. major*.

2. Materials and methods

2.1. Protein expression

The amplification of NDKb, ligation into the pET28a vector (Novagen, Madison, USA) and overexpression in *Escherichia coli* cells have been described previously (de Oliveira *et al.*, 2006). The NDKb clone is composed of 151 amino-acid residues with an additional sequence (MGSSHHHHHHSSGLVPRGSH) at the N-terminus comprising a 6×His tag, a thrombin site and a linker segment. Briefly, *E. coli* BL21 (DE3) pLysS strain transformed with pET28a-NDKb was inoculated into 1 l LB medium containing 34 µg ml^{-1} chloramphenicol and 35 µg ml^{-1} kanamycin and grown at 310 K to an OD_{600} of 0.6–0.7. Recombinant protein expression was induced by the addition of 0.6 m*M* isopropyl β-D-1-thiogalactopyranoside (IPTG; Promega) and the culture was incubated for an additional 5 h.

2.2. Protein purification

The cell pellet was resuspended in 40 ml lysis buffer (50 m*M* phosphate, 300 m*M* NaCl, 40 m*M* imidazole pH 8.0) containing 4 m*M* phenylmethylsulfonyl fluoride (PMSF; Sigma) and 1% Triton X-100, incubated for 30 min with 1 mg ml^{-1} lysozyme (Sigma) and the suspension was sonicated for 10 × 30 s (with 30 s intervals between each pulse) on ice. The sonicated cells were centrifuged at 10 000*g* for 30 min. The resulting cell-free extract was applied onto a HiTrap Chelating HP 5 ml column (GE Healthcare) previously equilibrated with lysis buffer using an ÄKTA fast protein liquid-chromatography (FPLC) system (GE Healthcare). Contaminant proteins were removed by washing with binding buffer containing 50 m*M* phosphate, 300 m*M* NaCl and 40 m*M* imidazole pH 8.0 at a flow rate of 1 ml min^{-1}. The bound fractions were eluted using a linear imidazole gradient from 0 to 0.5 *M* in the above buffer (the total elution volume was 100 ml) at a flow rate of 1 ml min^{-1}. The eluted protein was concentrated to 0.4 ml using an Amicon Ultra-4 10K centrifugal filter device (Millipore) and loaded onto a HiLoad 10/30 Superdex 75 (GE Healthcare) size-exclusion column pre-equilibrated with 10 m*M* MES buffer pH 6.0 containing 50 m*M* NaCl and 2 m*M* dithiothreitol (DTT) at a flow rate of 0.3 ml min^{-1}. Fractions containing the pure protein were pooled, concentrated to 10 mg ml^{-1}, flash-frozen in liquid nitrogen and stored at 193 K. The protein purity was estimated to be greater than 99% by SDS–PAGE analysis. The protein concentration was estimated by UV absorbance at 280 nm using a theoretical extinction coefficient of 22 585 M^{-1} cm^{-1}.

2.3. Dynamic light scattering

Dynamic light-scattering (DLS) measurements were carried out using a DynaPro 810 (Protein Solutions, Wyatt Technology Corporation) system equipped with a temperature-controlled microsampler. An autopilot run with 50 measurements every 20 s was used. Measurements were performed with protein solutions in 10 m*M* MES pH 6.0, 50 m*M* NaCl and 2 m*M* DTT at a constant temperature of 291 K and a protein concentration of 1 mg ml^{-1}. The samples to be analyzed were centrifuged and then filtered directly into the cuvette. The hydrodynamic parameters of purified NDKb were determined using the *Dynamics* v.6.3.40 software. The hydrodynamic radius ($R_{\rm h}$) was extrapolated from the translational diffusion coefficient ($D_{\rm t}$) using the Stokes–Einstein equation.

2.4. Crystallization

A protein solution at 10 mg ml^{-1} in 10 m*M* MES buffer pH 6.0 containing 50 m*M* NaCl and 2 m*M* DTT was used in the crystallization experiments. Crystallization experiments were performed by the sitting-drop vapour-diffusion method at 291 K using a Cartesian HoneyBee 963 system (Genomic Solutions). 928 conditions from commercially available crystallization kits from Hampton Research (SaltRX and Crystal Screens I and II), Emerald BioSystems (Precipitant Synergy and Wizard I and II) and Qiagen/Nextal (PACT, MPD, Ammonium Sulfate, Anions, Cations and JCSG+) were tested. Typically, 0.5 µl drops of protein solution were mixed with an equal volume of screening solution and equilibrated over a reservoir containing 0.08 ml of the latter solution. Initial crystallization setups

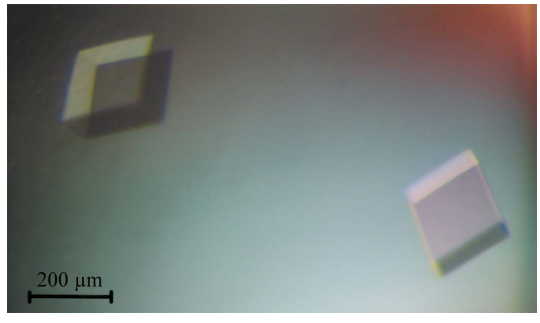

Figure 1
Microphotography of *L. major* NDKb crystals obtained using 100 m*M* citrate–HCl pH 5.6 and 1850 m*M* ammonium sulfate.

yielded microcrystals in four conditions. However, only one condition, containing ammonium sulfate as the precipitant, resulted in well shaped crystals. For crystal optimization, a systematic grid refinement was employed by varying the precipitant concentration from 1500 to 2200 m*M* in steps of 50 m*M*. Single crystals with approximate dimensions of 0.2 × 0.2 × 0.1 mm were obtained using a solution containing 100 m*M* citrate–HCl pH 5.6 and 1850 m*M* ammonium sulfate (Fig. 1). The crystals attained their maximum dimensions in 5–7 d.

2.5. X-ray diffraction analysis

For data collection, the NDKb crystal was soaked in a cryoprotectant solution [100 m*M* citrate–HCl pH 5.6, 1850 m*M* ammonium sulfate and 20%(*v*/*v*) glycerol] for 30 s and then flash-cooled in a nitrogen-gas stream at 100 K. X-ray diffraction data were collected on the W01B-MX2 beamline at the Brazilian Synchrotron Light Laboratory (Campinas, Brazil). The wavelength of the radiation source was set to 1.458 Å and a MARMosaic 225 mm CCD detector was used to record the X-ray diffraction data. The beam size was 0.3 × 0.3 mm and the crystal-to-detector distance was set to 140 mm. For each image, the exposure time was 80 s and the oscillation angle was 1°. A total of 180 images were collected. The data were indexed, integrated and scaled using the *DENZO* and *SCALEPACK* programs from the *HKL*-2000 package (Otwinowski & Minor, 1997). Data-processing statistics are summarized in Table 1. Molecular replacement was carried out using the program *AMoRe* (Navaza, 1994) and a model based on the atomic coordinates of nm23-H2 from *Homo sapiens* (PDB code 1nsk; Webb *et al.*, 1995).

3. Results and discussion

The full-length NDKb gene from *L. major* including the additional amino-acid sequence MGSSHHHHHHSSGLVPRGSH was over-expressed and purified to obtain a crystal-grade sample with high chemical purity and low structural polydispersity. Dynamic light-scattering (DLS) experiments indicated a monodispersive state (13.5% polydispersity) with an extrapolated hydrodynamic radius of 4.3 nm, which corresponds to a molecular weight of 105 kDa, using a calibration curve based on the diffusion coefficients of globular proteins. Taking into account the molecular weight of the monomer (18 675 Da), the calculated molecular weight from DLS experiments indicated that the protein is present as a hexamer in solution. The discrepancy between the estimated molecular weight from DLS experiments (105 kDa) and the expected hexamer weight from the sequence (112 kDa) can be attributed to the presence of a 6×His tag in the recombinant protein. The best quality crystals grew after 5–7 d in a 1:1 mixture of protein solution and 1850 m*M* ammonium sulfate (100 m*M* citrate–HCl buffer pH 5.6). A single crystal with dimensions of 0.25 × 0.25 × 0.15 mm (Fig. 1) was used for X-ray diffraction experiments and data were collected to 2.18 Å resolution (Fig. 2) under cryogenic conditions (100 K). A full 180° data set was collected using a crystal-to-detector distance of 140 mm with 1° oscillation and 80 s exposure per image. The reflections were indexed in the trigonal crystal system with unit-cell parameters a = 114.2, c = 93.9 Å and belonged to point group 32. An examination of the systematic absences indicated that the NDKb crystal belonged to either space group $P3_121$ or its enantiomorph $P3_221$. Calculation of the Matthews coefficient (Matthews, 1968) based on the molecular weight of 18 675 Da resulted in a V_M of 3.16 Å^3 Da^{-1} and a solvent content of 61.06%, which correspond to the presence of three molecules per asymmetric unit. The statistics of the data processing are summarized in Table 1. Molecular replacement (MR) was carried out with the program *AMoRe* (Navaza, 1994) using the atomic coordinates of nm23-H2, a human nucleoside diphosphate kinase b (PDB code 1nsk; Webb *et al.*, 1995), as a search model. The molecular-replacement calculations were performed in both of the enantiomorphic space groups $P3_121$ and $P3_221$ and the correlation coefficients from the translation-function calculations yielded an unambiguous solution in $P3_221$. Rigid-body refinement of the best MR solution for the three molecules in the resolution range 40.0–3.0 Å resulted in a correlation coefficient of 60.1% and an R factor of 39.4%. Isotropic and restrained refinement with *REFMAC*5 (Murshudov *et al.*, 1997) and manual model building using *Coot* (Emsley & Cowtan, 2004) are currently in progress. In parallel with crystallographic studies, SAXS and analytical ultracentrifugation experiments are being carried out in order to characterize the oligomeric state in solution of NDKb from *L. major*. NDKb plays a key role in the purine-salvage pathway in all trypanosomatid protozoa and the determination of its three-dimensional structure will be instrumental in understanding the biology of parasitic trypanosomatids and in the further development of new treatments for leishmaniasis.

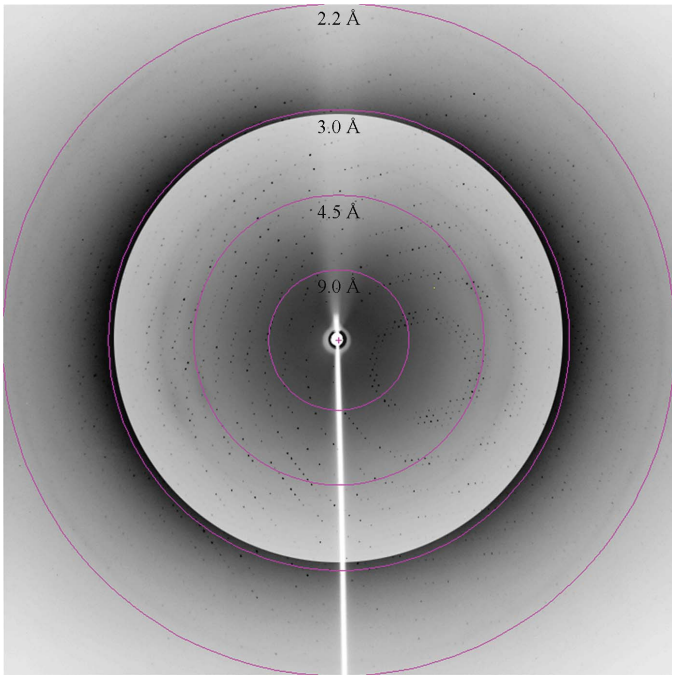

Figure 2
X-ray diffraction pattern of the *L. major* NDKb crystal with a different contrast level at low and high resolutions. The purple circles show resolution ranges of 9.0, 4.5, 3.0 and 2.2 Å, respectively.

We gratefully thank the Center for Structural Molecular Biology (ABTLuS, Campinas, Brazil) and the Brazilian Synchrotron Light Laboratory (ABTLuS, Campinas, Brazil) for provision of the automated crystallization laboratory (RoboLab) and synchrotron-radiation facilities (beamline W01B-MX2), respectively. This research was supported by grants from FAPESP (07/06755-2) to AHCO, FAPESP (07/54865) and CNPq (307853/2006-3, 473997/2007-0) to RKA and CNPq (471192/2007-4) to MTM.

References

Chakrabarty, A. M. (1998). *Mol. Microbiol.* **28**, 875–882.
Emsley, P. & Cowtan, K. (2004). *Acta Cryst.* D**60**, 2126–2132.

Gounaris, K., Thomas, S., Najarro, P. & Selkirk, M. E. (2001). *Infect. Immun.* **69**, 3658–3662.
Jeudy, S., Lartique, A., Claverie, J. M. & Abergel, C. (2009). *J. Virol.* **83**, 7142–7150.
Kolli, B. K., Kostal, J., Zaborina, O., Chakrabarty, A. M. & Chang, K. (2008). *Mol. Biochem. Parasitol.* **158,** 163–175.
Lacombe, M. L., Sastre-Garau, X., Lascu, I., Vonica, A., Wallet, V., Thiery, J. P. & Véron, M. (1991). *Eur. J. Cancer*, **27**, 1302–1307.
Landfear, S. M., Ullman, B., Carter, N. S. & Sanchez, M. A. (2004). *Eukaryot. Cell*, **3**, 245–254.
Lascu, I., Giartosio, A., Ransac, S. & Erent, M. (2000). *J. Bioenerg. Biomembr.* **32**, 227–236.
Marr, J. J. (1991). *Biochemical Protozoology*, edited by G. H. Coombs & M. J. North, pp. 525–536. London: Taylor & Francis.
Matthews, B. W. (1968). *J. Mol. Biol.* **33**, 491–497.
Murshudov, G. N., Vagin, A. A. & Dodson, E. J. (1997). *Acta Cryst.* D**53**, 240–255.
Misra, G., Aggarwal, A., Dube, D., Zaman, M. S., Singh, Y. & Ramachandran, R. (2009). *Proteins*, **76**, 496–506.
Navaza, J. (1994). *Acta Cryst.* A**50**, 157–163.
Oliveira, A. H. C. de, Cruz, A. K., Ruiz, J. C., Greene, L. J., Rosa, J. C. & Ward, R. J. (2006). *Comp. Biochem. Physiol. D*, **3**, 300–308.
Otwinowski, Z. & Minor, W. (1997). *Methods Enzymol.* **276**, 307–326.
Parks, R. E. Jr & Agarwal, R. P. (1973). *The Enzymes*, edited by P. D. Boyer, Vol. 8, pp. 307–334. New York: Academic Press.
Postel, E. H. (2003). *J. Bioenerg. Biomembr.* **35**, 31–40.
Punj, V., Zaborina, O., Dhiman, N., Falzari, K., Bagdasarian, M. & Chakrabarty, A. M. (2000). *Infect. Immun.* **68**, 4930–4937.
Shankar, S., Kamath, S. & Chakrabarty, A. M. (1996). *J. Bacteriol.* **178**, 1777–1781.
Webb, P. A., Perisic, O., Mendola, C. E., Backer, J. M. & Williams, R. L. (1995). *J. Mol. Biol.* **251**, 574–587.
Zaborina, O., Misra, N., Kostal, J., Kamath, S., Kapatral, V., El-Idrissi, M. E., Prabhakar, B. S. & Chakrabarty, A. M. (1999). *Infect. Immun.* **67**, 5231–5242.